Journal of Magnetic Resonance **143,** 431–434 (2000)
doi:10.1006/jmre.2000.2048, available online at http://www.idealibrary.com on IDEAL®

^{3h}J Coupling between C^{α} and H^{N} across Hydrogen Bonds in Proteins

Axel Meissner and Ole Winneche Sørensen

Department of Chemistry, Carlsberg Laboratory, Gamle Carlsberg Vej 10, DK-2500 Valby, Denmark

Received December 30, 1999; revised February 2, 2000

***J* couplings between $^{13}C^{\alpha}$ and $^{1}H^{N}$ across hydrogen bonds in proteins are reported for the first time, and a two- or three-dimensional NMR technique for their measurement is presented. The technique exploits the TROSY effect, i.e., the degree of interference between dipolar and chemical shift anisotropy relaxation mechanisms, for sensitivity enhancement. The 2D or 3D spectra exhibit E.COSY patterns where the splittings in the ^{13}CO and $^{1}H^{N}$ dimensions are $^{1}J(^{13}C^{\alpha}, ^{13}CO)$ and the desired $^{3h}J(^{13}C^{\alpha}, ^{1}H^{N})$, respectively. A demonstration of the new method is shown for the $^{15}N,^{13}C$-labeled protein chymotrypsin inhibitor 2 where 17 $^{3h}J(^{13}C^{\alpha}, ^{1}H^{N})$ coupling constants ranging from 0 to 1.4 Hz where identified and all of positive sign.** © 2000 Academic Press

Key Words: ^{h}J; $^{3h}J(^{13}C^{\alpha}, ^{1}H^{N})$; **hydrogen bonds; TROSY; E.COSY.**

J couplings across hydrogen bonds in biomolecules have within a short period of time become very important constraints for structure determination of biological macromolecules by NMR spectroscopy. The *J* coupling constants across hydrogen bonds observed so far (*1–9*) are between the three spin-$\frac{1}{2}$ nuclei intimately involved with the hydrogen bond, e.g., in a protein ^{15}N, $^{1}H^{N}$, and ^{13}CO.

In this Communication, we report for the first time observation of ^{3h}J coupling constants between $^{13}C^{\alpha}$ and $^{1}H^{N}$ across hydrogen bonds in a protein. The pulse sequence developed for this purpose is outlined in Fig. 1. It is of the three-dimensional (3D) ^{h}HNCO TROSY type and similar to an earlier sequence for measurement of $^{2h}J(^{13}CO, ^{1}H^{N})$ in proteins (*9*) but no $^{13}C^{\alpha}$ decoupling is applied during ^{13}CO evolution. This is in order to generate a spectrum where $^{1}J(^{13}CO, ^{13}C^{\alpha})$ serves as a large coupling constant in the $\{^{13}CO, ^{13}C^{\alpha}, ^{1}H^{N}\}$ triple of spins allowing E.COSY (*10–12*) measurement of $^{3h}J(^{13}C^{\alpha}, ^{1}H^{N})$.

The sequence starts by directing the native $^{1}H^{N}$ and ^{15}N magnetizations into the ^{15}N TROSY resonance that evolves during a relatively long delay *T* (typically $2/^{1}J(^{13}CO, ^{15}N)$) for building up antiphase magnetization with respect to ^{13}CO across the hydrogen bond via $^{3h}J(^{13}CO, ^{15}N)$. Then magnetization transfer from ^{15}N to ^{13}CO takes place by a pair of $\pi/2$ pulses and the t_1 evolution period with ^{13}CO magnetization under $^{13}C^{\alpha}$-coupled and ^{15}N-decoupled conditions follows. During this period there is a relatively large frequency separation, $^{1}J(^{13}CO, ^{13}C^{\alpha})$, between the components corresponding to the α and β spin states of $^{13}C^{\alpha}$. Hence by not perturbing $^{13}C^{\alpha}$ in the rest of the pulse sequence apart from possible π pulses, the resonances corresponding to $^{13}C^{\alpha}$ in the α and β spin states in the $^{1}H^{N}$ dimension are separated in an E.COSY manner. In the back transfer from ^{13}CO to $^{1}H^{N}$ for detection a TROSY mixing sequence (*13–15*) is employed for the final magnetization transfer from ^{15}N to $^{1}H^{N}$ but the E.COSY measurement of $^{3h}J(^{13}C^{\alpha}, ^{1}H^{N})$ is independent thereof. However, because of the rather long delays with transverse ^{15}N magnetization the TROSY approach offers the highest sensitivity at high fields even for small proteins exhibiting modest TROSY effects.

The second long delay *T* serves as a constant-time evolution period in the 3D version of the pulse sequence where the $^{13}C^{\alpha}$ π pulse for suppression of the $^{1}J(^{13}C^{\alpha}, ^{15}N)$ and $^{2}J(^{13}C^{\alpha}, ^{15}N)$ coupling constants is a critical element. If it affects the ^{13}CO spins, refocusing of $^{3h}J(^{13}CO, ^{15}N)$ prior to the $^{15}N \rightarrow ^{1}H$ TROSY element will be compromised and the sensitivity reduced. If it is imperfect in inverting the $^{13}C^{\alpha}$ spins, the E.COSY patterns will be corrupted and the pertinent peak separations will be smaller than the actual $^{3h}J(^{13}C^{\alpha}, ^{1}H^{N})$ coupling constants (*16*). Hence we prefer to leave out this $^{13}C^{\alpha}$ π pulse and consequently not suppress $^{1}J(^{13}C^{\alpha}, ^{15}N)$ and $^{2}J(^{13}C^{\alpha}, ^{15}N)$ in the ^{15}N dimension which thereby puts a lower limit of about 25 Hz for the meaningful digital resolution in that dimension. Another detail of the pulse sequence concerns the gradient delays δ that were not present in the originally developed TROSY pulse sequence (*13*) but was introduced (*14, 15*) to enable formation of heteronuclear gradient echoes to improve solvent and artifact suppression. In the 2D TROSY sequence formation of gradient echoes require three such delays δ but in ^{h}HNCO TROSY and also in conventional HNCO TROSY the overall duration of the pulse sequence is only prolonged by a single δ delay.

An experimental demonstration of the ^{h}HNCO pulse sequence without $^{13}C^{\alpha}$ decoupling is shown in Fig. 2 with a 2D projection of a spectrum of $^{15}N,^{13}C$-labeled chymotrypsin inhibitor 2 19–83 (CI2) (*17*) expressed, purified, and $^{15}N,^{13}C$-labeled as described previously (*18, 19*). A total of 17 cross peaks representing the same number of nonvanishing $^{3h}J(^{13}CO, ^{15}N)$ coupling constants across hydrogen bonds are observed. This is about half of the hydrogen bonds reported in Ref. (*17*). Three of them are between separate secondary structures while the rest are within α helix, beta sheet, or turns (*17*).

From the E.COSY patterns of the cross peaks with separa-

1090-7807/00 $35.00

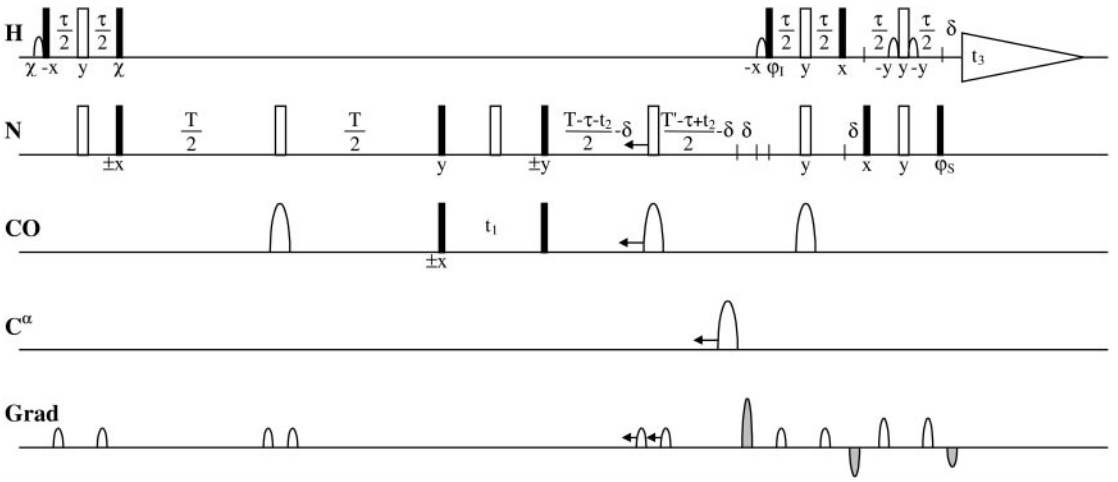

FIG. 1. 3D ^{h}HNCO TROSY pulse sequence for measurement of $^{3h}J(^{13}C^{\alpha}, {}^{1}H^{N})$ coupling constants. Filled and open bars represent $\pi/2$ and π pulses, respectively. Selective $\pi/2$ water pulses and selective π carbon pulses are shown as open bell shapes. $\tau = (2J_{N,H})^{-1}$; $T = n(^{1}J_{N,CO})^{-1}$, $n = 1, 2, \ldots$; $T' = T - 2$ (length of selective water $\pi/2$ pulse); δ = gradient delay. In the Watergate element the duration of the selective pulses are included in the τ delay. The pulse phases are indicated below the pulses. Pulse phases with the prefix $\pm$ indicate independent two-step phase cycles with alternating receiver phase. In order to include the native *S* spin magnetization in the TROSY resonance, the phase χ must be $-y$ on our Varian Unity Inova spectrometers while it must be y on our Bruker DRX 600 instrument. States–TPPI is applied on the $\pi/2$ pulse before t_1. In t_2/t_3 echo and antiecho data sets are recorded in combination with the shaded pulsed field gradients of relative strengths −4.375:1.875:1.250 for echo and −5.000:1.250:1.875 for antiecho selection. The other gradients are arranged in self-compensating pairs. The phase settings for echo and antiecho on the Varian instruments are $\{\varphi_I = y; \varphi_S = y\}$ and $\{\varphi_I = -y; \varphi_S = -y\}$, respectively, while it would be reversed on the Bruker instrument. In the 2D version of the experiment (i.e., $t_2 = 0$) the $^{13}C^{\alpha}$ π pulse is omitted which often is also the case in 3D applications (see text).

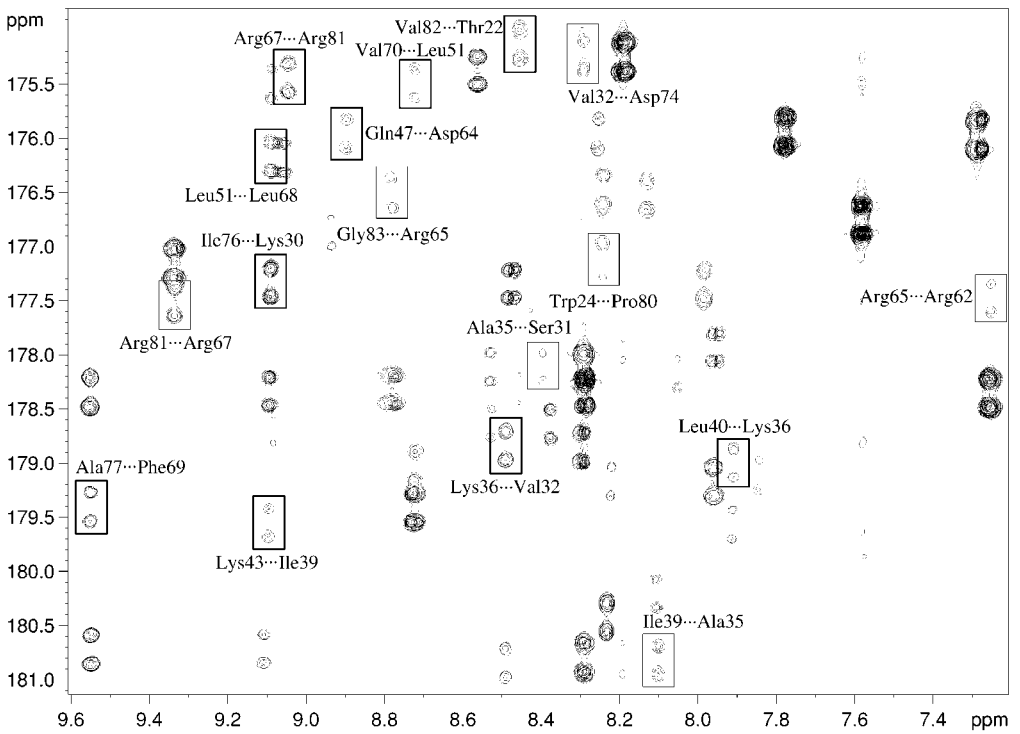

FIG. 2. 2D projection of selected F_1/F_3 planes from a 3D ^{h}HNCO TROSY spectrum of ^{15}N,^{13}C-labeled CI2 19−83 (90% H_2O/10% D_2O, 25°C, pH 4.2, 18 mg in 300 μl) recorded on a Varian Unity Inova 800 MHz spectrometer in about 4 $\frac{1}{2}$ days. The hydrogen bond correlation cross peaks are all framed and those in boldface are expanded in Fig. 3. Parameters: relaxation delay 1.5 s, T = 133.3 ms; T' = 132.3 ms; τ = 5.43 ms; t_1(max) = 59.0 ms (initial t_1 = 0.5 ms); t_2(max) = 9.0 ms; t_3(max) = 91.4 ms; 16 scans. Sinc (*20*) shaped selective water pulses (1000.0 μs) and iBurp (*21*) shaped selective carbon pulses (930.0 μs) were used. Rectangular $\pi/2$ ^{13}CO pulses were calibrated to have a zero excitation profile in the C^{α} region. The open gradients in Fig. 1 had relative amplitudes of 0.8 in the initial INEPT transfer, 1.0 in the T periods, 1.0 in the first S^3CT element of TROSY transfer, and 6.0 in the final S^3CT/Watergate element. Data matrices of 236 × 56 × 2048 points covering 2000 × 3000 × 12,000 Hz were zero-filled to 512 × 64 × 4096 prior to Fourier transformation and the window functions were cosine in all three dimensions. Linear back prediction of 2 data points was applied in t_1 using 80 coefficients to avoid phase correction in this dimension. Boxes in the spectrum indicate the 17 observed cross peaks from $^{1}H^{N}$–^{13}CO correlations across hydrogen bonds.

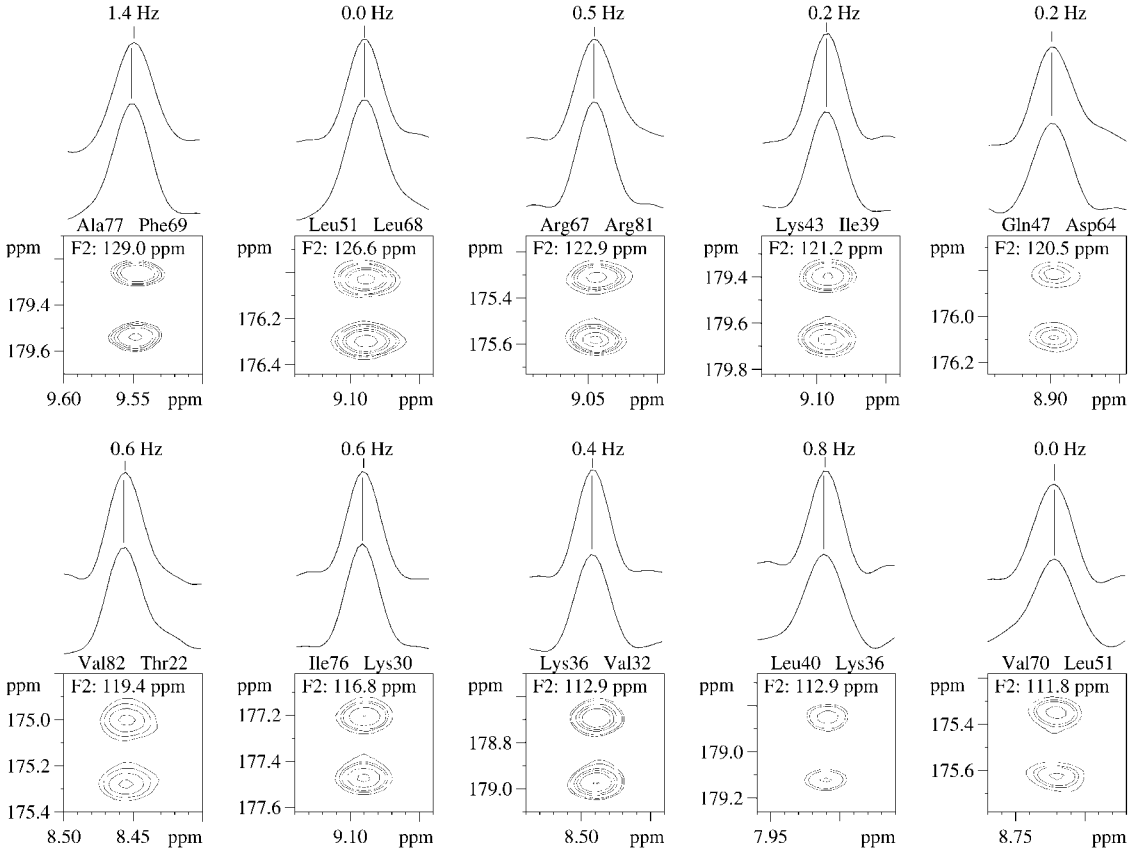

FIG. 3. Expansion of the boldface boxes in the 3D ^{h}HNCO TROSY spectrum in Fig. 2 showing $^{1}H^{N}$–^{13}CO correlations across hydrogen bonds along with appropriate 1D F_3 sections through the center of the peaks. The ^{15}N chemical shifts in the F_2 dimension are indicated in the 2D planes. Cross peak components are separated by $^{1}J(^{13}CO, ^{13}C^{\alpha})$ in the F_1 dimension and their displacement in the F_3 dimension represents $^{3h}J(^{13}C^{\alpha}, ^{1}H^{N})$.

tions $^{1}J(^{13}CO, ^{13}C^{\alpha})$ and $^{3h}J(^{13}C^{\alpha}, ^{1}H^{N})$ in the F_1 and F_3 dimensions, respectively, the latter can be measured from appropriate sections as shown for selected examples in Fig. 3. The sign of $^{3h}J(^{13}C^{\alpha}, ^{1}H^{N})$ is in all cases positive and ranging between 0 and 1.4 Hz or possibly slightly higher for Trp24 · · · Pro80 that is more uncertain because of spectral overlap and lower sensitivity. We estimate the precision of the ^{h}J coupling constants measured in Fig. 3 to be about a quarter of a Hertz.

A recent study has concluded that there is proportionality between corresponding $^{3h}J(^{13}CO, ^{15}N)$ and $^{2h}J(^{13}CO, ^{1}H^{N})$ coupling constants in the protein ubiquitin (*8*). Our earlier measurement of $^{2h}J(^{13}CO, ^{1}H^{N})$ (*9*) and the measurement of $^{3h}J(^{13}C^{\alpha}, ^{1}H^{N})$ in the present study do not indicate that there should be a similar relationship between these two coupling constants. We take this as an indicator that $^{3h}J(^{13}C^{\alpha}, ^{1}H^{N})$ might contain independent structural information about the conformation around the hydrogen bond but clearly further data are necessary to determine the details of this correlation.

In conclusion, we have described a new method for measurement of $^{3h}J(^{13}C^{\alpha}, ^{1}H^{N})$ coupling constants across hydrogen bonds in proteins and observed these couplings for the first time. Further studies on different proteins are necessary to determine the correlation between $^{3h}J(^{13}C^{\alpha}, ^{1}H^{N})$ and the detailed structure around the hydrogen bond.

ACKNOWLEDGMENTS

The spectra presented were recorded on the Varian Unity Inova 800 MHz spectrometer of the Danish Instrument Center for NMR Spectroscopy of Biological Macromolecules at Carlsberg Laboratory. We thank Flemming M. Poulsen and Mathilde H. Lerche for the ^{15}N,^{13}C-labeled CI2 sample.

REFERENCES

1. A. J. Dingley and S. Grzesiek, *J. Am. Chem. Soc.* **120,** 8293–8297 (1998).
2. K. Pervushin, A. Ono, C. Fernandez, T. Szyperski, M. Kainosho, snd K. Wüthrich, *Proc. Natl. Acad. Sci. U.S.A.* **95,** 14147–14151 (1998).
3. A. J. Dingley, J. E. Masse, R. D. Peterson, M. Barfield, J. Feigon, and S. Grzesiek, *J. Am. Chem. Soc.* **121,** 6019–6027 (1999).
4. F. Cordier and S. Grzesiek, *J. Am. Chem. Soc.* **121,** 1601–1602 (1999).
5. G. Cornilescu, J.-S. Hu, and A. Bax, *J. Am. Chem. Soc.* **121,** 2949–2950 (1999).
6. G. Cornilescu, B. E. Ramirez, M. K. Frank, G. M. Clore, A. M. Gronenborn, and A. Bax, *J. Am. Chem. Soc.* **121,** 6275–6279 (1999).

7. Y.-X. Wang, J. Jacob, F. Cordier, P. Wingfield, S. J. Stahl, S. Lee-Huang, D. Torchia, S. Grzesiek, and A. Bax, *J. Biomol. NMR* **14,** 181–184 (1999).
8. F. Cordier, M. Rogowski, S. Grzesiek, and A. Bax, *J. Magn. Reson.* **140,** 510–512 (1999).
9. A. Meissner and O. W. Sørensen, *J. Magn. Reson.* **143,** 387–390 (2000).
10. C. Griesinger, O. W. Sørensen, and R. R. Ernst, *J. Am. Chem. Soc.* **107,** 6394–6395 (1985).
11. C. Griesinger, O. W. Sørensen, and R. R. Ernst, *J. Chem. Phys.* **85,** 6837–6852 (1986).
12. C. Griesinger, O. W. Sørensen, and R. R. Ernst, *J. Magn. Reson.* **75,** 474–492 (1987).
13. K. Pervushin, R. Riek, G. Wider, and K. Wüthrich, *Proc. Natl. Acad. Sci. U.S.A.* **94,** 12366–12371 (1997).
14. A. Meissner, T. Schulte-Herbrüggen, J. Briand, and O. W. Sørensen, *Mol. Phys.* **95,** 1137–1142 (1998).
15. M. Lerche, A. Meissner, F. M. Poulsen, and O. W. Sørensen, *J. Magn. Reson.* **140,** 259–263 (1999).
16. A. Meissner, T. Schulte-Herbrüggen, and O. W. Sørensen, *J. Am. Chem. Soc.* **120,** 7989–7990 (1998).
17. S. Ludvigsen, H. Shen, M. Kjær, J. C. Madsen, and F. M. Poulsen, *J. Mol. Biol.* **222,** 621–635 (1991).
18. P. Osmark, P. Sørensen, and F. M. Poulsen, *Biochemistry* **32,** 11007–11014 (1993).
19. J. C. Madsen, O. W. Sørensen, P. Sørensen, and F. M. Poulsen, *J. Biomol. NMR* **3,** 239–244 (1993).
20. A. J. Temps and C. F. Brewer *J. Magn. Reson.* **56,** 355–372 (1984).
21. H. Geen and R. Freeman *J. Magn. Reson.* **93,** 93–141 (1991).